

Exotic phase transition and superconductivity in layered titanium-oxypnictides implied by a computational phonon analysis

Kousuke Nakano^{1,*}, Kenta Hongo^{1,2,3}, and Ryo Maezono^{1†}

¹ School of Information Science, JAIST, Asahidai 1-1, Nomi, Ishikawa 923-1292, Japan,

² JST-PRESTO, 4-1-8 Honcho, Kawaguchi, Saitama 332-0012, Japan, and

³ Center for Materials research by Information Integration (CM²),
National Institute for Materials Science (NIMS), 1-2-1 Sengen, Tsukuba, Ibaraki 305-0047, Japan

(Dated: February 3, 2017)

We applied *ab initio* phonon analysis to layered titanium-oxypnictides, $\text{Na}_2\text{Ti}_2\text{Pn}_2\text{O}$ ($\text{Pn} = \text{As}, \text{Sb}$), and found a clear contrast between the cases with lighter/heavier pnictogen in comparisons with experiments. The result completely explains the experimental structure, $C2/m$ for $\text{Pn} = \text{As}$, within the conventional electron-phonon framework, while there arise discrepancies when the pnictogen gets heavier, being in the same trend for the $\text{BaTi}_2\text{Pn}_2\text{O}$ ($\text{Pn} = \text{As}, \text{Sb}, \text{Bi}$) case. The fact implies a systematic dependence on pnictogen to tune the mechanism of the phase transition and superconductivity from conventional to exotic.

PACS numbers: 71.45.Lr, 74.25.Kc, 74.70.-b

I. INTRODUCTION

Recently discovered layered titanium-oxypnictides, $\text{ATi}_2\text{Pn}_2\text{O}$ [$A = \text{Na}_2, \text{Ba}, (\text{SrF})_2, (\text{SmO})_2$; $\text{Pn} = \text{As}, \text{Sb}, \text{Bi}$] [1–12], is a new superconducting family, and their superconducting mechanisms have attracted intensive attentions because their crystal and electronic structures are similar to the exotic superconductors such as cuprates [13] or iron arsenides [14]. The mechanism has been expected to be *conventional*, namely electron-phonon driven [15–18], and accompanying singularities in resistivity and susceptibility at low temperature are regarded due to the conventional charge density wave (CDW) [16–20]. Recent works are, however, pointing out the possibility of *exotic* mechanism for these compounds: For $\text{BaTi}_2\text{Pn}_2\text{O}$ ($\text{Pn} = \text{As}, \text{Sb}$), Frandsen *et al.* reported the breaking four-fold symmetry at low temperature without any superlattice peaks by Neutron diffraction and TEM [21], and suggested the possibility of the intra-unit-cell nematic CDW [22, 23] to make account for the breaking. A theoretical suggestion was made that such an intra-unit-cell nematic CDW could be realized by the orbital ordering mediated by spin-fluctuations [24]. The Uemura classification scheme [25] also supports exotic superconducting mechanisms in these compounds [26]. Though our latest phonon evaluations [27] partly refuted that the breaking could be explained within the conventional electron-phonon mechanism at least for $\text{Pn} = \text{As}$, it is still unknown if this is the case for $\text{Pn} = \text{Sb}$ and Bi , leaving debates about whether the mechanism is conventional or exotic.

Examining whether the observed superlattices are explained by the conventional *ab initio* framework or not can provide a critical clue for the questions. For experimental side, Davies *et al.* [28] have just synthesized large single crystals of $\text{Na}_2\text{Ti}_2\text{Pn}_2\text{O}$ ($\text{Pn} = \text{As}, \text{Sb}$) (Fig. 1) in order to achieve reliable diffraction measurements, and observed clear superlattice

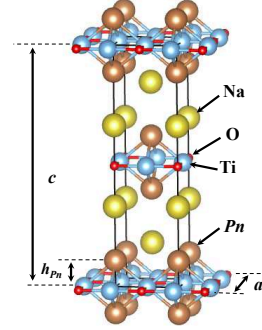


FIG. 1. The crystal structure of $\text{Na}_2\text{Ti}_2\text{Pn}_2\text{O}$ ($\text{Pn} = \text{As}, \text{Sb}$). The space group is $I4/mmm$.

peaks of $2 \times 2 \times 2$ and $2 \times 2 \times 1$ for $\text{Pn} = \text{As}$ and Sb , respectively. For $\text{Pn} = \text{As}$, a recent phonon calculation[29] reported possible superlattices but they could not explain the observed peaks. In this paper, we report that our *ab initio* phonon calculations can explain the observed $C2/m$ (monoclinic No.12) structure for $\text{Pn} = \text{As}$, implying that the conventional electron-phonon driven mechanism is likely for this system. For $\text{Pn} = \text{Sb}$, on the other hand, we obtained $Cmce$ (Orthorhombic No.64) superlattice, being inconsistent with the observed one [$Cmcm$ (Orthorhombic No.63)]. The discrepancy would support exotic mechanisms likely for $\text{Pn} = \text{Sb}$ in contrast. Based on the results combined with preceding studies[15, 27, 30–33], we propose a new possibility that a heavier Pn causes stronger electron correlations and induces exotic phase transition and superconductivity that cannot be explained by the conventional framework.

II. METHOD

All the calculations were done within DFT using GGA-PBE exchange-correlation functionals [34], implemented in Quantum Espresso package. [35] We adopted PAW [36] pseudo potentials. The present PAW implementation takes

* kousuke_1123@icloud.com

† rmaezono@mac.com

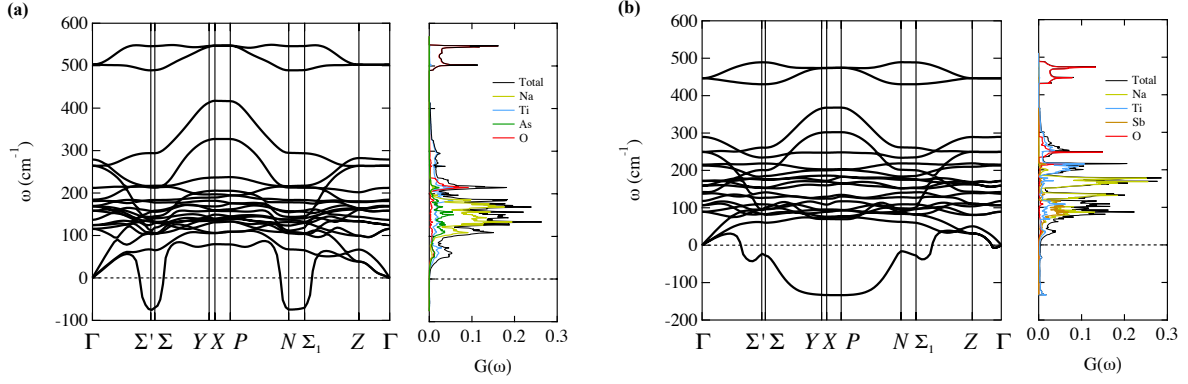


FIG. 2. Phonon dispersions and phonon DOS for undistorted ($I4/mmm$) $\text{Na}_2\text{Ti}_2\text{Pn}_2\text{O}$ ($Pn =$ (a) As, (b) Sb). The primitive Brillouin zones are shown in Fig. 7 (a)

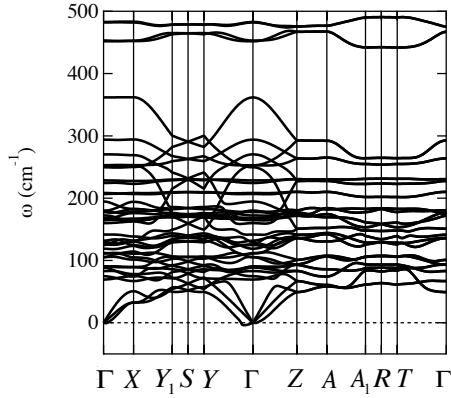


FIG. 3. Phonon dispersions for $\text{Na}_2\text{Ti}_2\text{Sb}_2\text{O}$ superlattice ($Cmce$). The primitive Brillouin zone is shown in Fig. 7 (b).

into account the scalar-relativistic effects upon a careful comparison with all-electron calculations. [37, 38] We restricted ourselves to spin unpolarized calculations. Lattice instabilities were detected by the negative (imaginary) phonon dispersions evaluated for undistorted and distorted structures. Taking each of the negative phonon modes, the structural relaxations along the mode were evaluated by the BFGS optimization scheme with the structural symmetries fixed to $C2/m$ for $\text{Na}_2\text{Ti}_2\text{As}_2\text{O}$, $Cmce$ for $\text{Na}_2\text{Ti}_2\text{Sb}_2\text{O}$. For phonon calculations, we used the linear response theory implemented in Quantum Espresso package. [39] Crystal structures and Fermi surfaces were depicted by using VESTA [40] and XCrySDen [41], respectively.

To deal with all the compounds systematically, we checked the convergence of plane-wave cutoff energies (E_{cut}), k -meshes, q -meshes, and smearing parameters. The most strict condition among the compounds was taken to achieve the convergence within ± 1.0 mRy per formula unit in the ground state energy, resulting in $E_{\text{cut}}^{(\text{WF})} = 90$ Ry for wavefunction

and $E_{\text{cut}}^{(\rho)} = 800$ Ry for charge density. For undistorted $\text{Na}_2\text{Ti}_2\text{As}_2\text{O}$ and $\text{Na}_2\text{Ti}_2\text{Sb}_2\text{O}$, $(6 \times 6 \times 6)$ k -meshes were used for the Brillouin-zone integration. Phonon dispersions were calculated on $(6 \times 6 \times 6)$ q -meshes. For distorted $\text{Na}_2\text{Ti}_2\text{As}_2\text{O}$ ($C2/m$) and $\text{Na}_2\text{Ti}_2\text{Sb}_2\text{O}$ ($Cmce$) superlattices, $(4 \times 4 \times 4)$ k -meshes were used. For the distorted $\text{Na}_2\text{Ti}_2\text{Sb}_2\text{O}$ superlattice, $(4 \times 4 \times 4)$ q -meshes were used to calculate phonon dispersions. We also calculated a ground state energy of the experimentally observed $\text{Na}_2\text{Ti}_2\text{Sb}_2\text{O}$ ($Cmcm$) superlattice [28] with $(6 \times 6 \times 3)$ k -meshes. The Marzari-Vanderbilt cold smearing scheme [42] with a broadening width of 0.01 Ry was applied to all the compounds. All the calculations were performed with the primitive lattices.

III. RESULTS AND DISCUSSION

Figure 2 (a) shows the phonon dispersions for $Pn = \text{As}$, giving imaginary frequencies appearing around $N = (2\pi/a) \cdot (1/2, 0, a/c)$ and $\Sigma' = (2\pi/a) \cdot (1/2, 0, 0)$, where a and c are conventional lattice constants for the undistorted structure. The compatible modes with the experimental observation [28] that the twice larger periodicity along c -axis realized are $N = (2\pi/a) \cdot (1/2, 0, a/c)$ and $N' = (2\pi/a) \cdot (0, 1/2, a/c)$. We note that the previous phonon calculation [29] could not reproduce this doubled periodicity. We therefore took these for further lattice relaxations from the original $I4/mmm$ structure along the mode displacements to get $C2/m$ (monoclinic, No.12) superlattice (Fig. 4 (a) and Fig. 5 (a)), being consistent with the experiments [28]. The resultant optimized geometry after the relaxation gives fairly good agreement with the experiments [28] within deviations at most 2.5% (See Appendix C). We could not confirm whether or not the negative modes disappear in the $C2/m$ superlattice just because of intractable computational costs for enlarged reciprocal space by the lowered symmetry.

For $Pn = \text{Sb}$, we obtained phonon dispersions as shown in Fig. 2 (b). Imaginary frequencies appear widely around $X = (2\pi/a) \cdot (1/2, 1/2, 0)$ and $P = (2\pi/a) \cdot (1/2, 1/2, a/2c)$. The

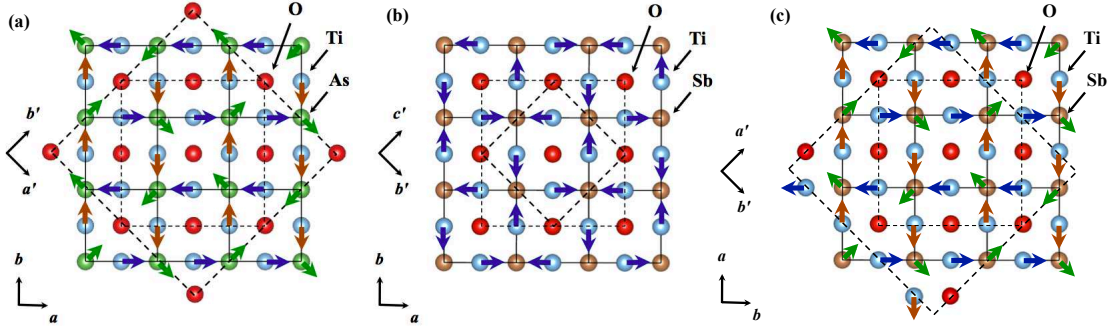


FIG. 4. In-plane superlattice structures obtained by our calculations for $Pn =$ (a) As and (b) Sb, and (c) the observed in-plane superlattice structure for $Pn =$ Sb [28]. Pn is located above and below the Ti_2O plane. Solid lines represent the original unit cells for $I4/mmm$. Thin dash lines represent the unit cells for 2×2 superlattices. Solid dash lines represent redefined unit cells for distorted superlattices.

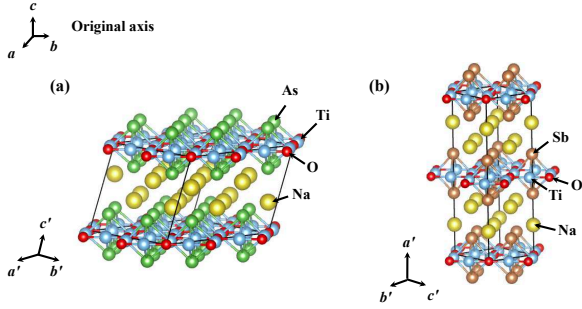


FIG. 5. 3D superlattice structures obtained from our calculations for $Pn =$ (a) As ($C2/m$) and (b) Sb ($Cmce$).

experiments [28] reported that the twice larger super periodicity is realized only in ab -plane, not along c -axis. It is therefore X mode being likely to realize the instability toward the superlattice. By optimizing the geometry along the mode displacement, we obtained $Cmce$ (orthorhombic, No.64) (Fig. 4 (b) and Fig. 5 (b)), being inconsistent with the observed $Cmcm$ (orthorhombic, No.63) structure (Fig. 4 (c)) in the experiment[28]. To confirm the present conclusion further, we examined the stability by seeing if the imaginary frequencies disappear at the relaxed structure, as shown in Fig. 3. In addition to confirming the stability, we compared enthalpies between our $Cmce$ and the observed $Cmcm$. The optimized geometry with $Cmce$ is found to be more stable by 11 mRy per formula unit than that with $Cmcm$. These results mean that the experimentally observed $Cmcm$ is energetically unfavorable within DFT framework.

Putting the discrepancy for $Pn =$ Sb aside for a while, we can provide a plausible explanation for the lattice instabilities as follows: The lattice instability mainly derives from in-plane Ti vibration. To make account for the inter-atomic forces to restore the lattice displacements, we can ignore (at least for the discussion of the instability) the contribution from Na because there are no bonds between Na and Ti (Fig. 1). Starting with X mode for $Pn =$ Sb (Fig. 4 (b)), it generates a displace-

ment such that a rectangular formed by Ti rotates to vibrate within ab -plane. A possible restoring force would come from inter-ion interactions between Ti^{3+} and nearest O^{2-} , but the force is orthogonal to the displacement and hence we can ignore it. Primary force would therefore come from Ti- Pn interaction for Ti approaching to Pn when the rectangular rotates. The trend in the electronegativity (As = 2.18, Sb = 2.05) implies a weaker Ti- Pn interaction for $Pn =$ Sb. The fact that we get the instability only for $Pn =$ Sb implies that the threshold would be around 2.1 in terms of the electronegativity against the instability. For N mode (Fig. 4 (a)), the imaginary frequency appears commonly for $Pn =$ As and Sb. This is also accountable along the above discussion. In this mode, the Ti- Pn interaction has little effect on the restoring forces because Ti and Pn move in the same direction. The possible restoring force would originate from nearest Oxygen and again this is orthogonal to the displacement, giving too weak contribution leading to the instability. This is the reason why the imaginary frequencies appear at N mode for both Pn .

Getting back to the discrepancy, the present results confront the sharp contrast between $Pn =$ As and Sb in terms of whether the conventional electron-phonon treatment for the phase transition works or not. Since it is clearly reported [28] that the measured XRD results cannot be identified by the $\sqrt{2} \times \sqrt{2} \times 1$ superlattice (Fig. 4 (b)), the discrepancy would be intrinsic so that it should be accounted for by those mechanism beyond the conventional ones, such as strong electronic correlations. As discussed above, the present predictions about the instabilities even including $Pn =$ Sb can be explained to some extent by a plausible physical picture, but another mechanism could dominate over this to critically decide which mode is chosen as the phonon condensation mode when the temperature decreases.

One of the possible mechanisms would be the spatial anisotropy introduced via spin-orbit couplings [43] under the enhanced polarizations by the electronic correlation: [30, 31] In layered titanium-oxypnictides, the hybridization between Ti-3d and p -orbitals of Pn [15, 27, 32, 33] is one of the critical factor for the transport property about how much the va-

lence electrons are localized. For iron arsenide superconductors, such tendency toward the localization is well captured by the trend of h , the vertical distances between Fe layer and Pn or Ch [30, 31] (Fig. 1). When h gets larger, the covalency gets weaker to make Fe-3d more localized and then the spin/orbital polarizations get enhanced as one of the electronic correlation effect. [30, 31] If we apply the similar analysis to the present case, we get $h_{Pn=Bi} > h_{Pn=Sb} > h_{Pn=As}$ [4–7, 44, 45] for the experimental geometry. This trend would support the correlation effect gets more enhanced for Sb than As.

The trend in h above is again consistent with our previous study for $BaTi_2Pn_2O$ ($Pn = As, Sb, Bi$), where we showed that the conventional electron-phonon framework could explain experiments only for $Pn = As$, but not for the other heavier Pn . [27] It might be a general tendency also applicable to the layered titanium-oxypnictides that the larger h enhances the electronic correlations as the origin of the exotic mechanism. Such mechanisms have actually been proposed by several authors [24, 43] such as the phase transition driven not by CDW but by the orbital ordering [43], or the orbital ordering induced by spin-fluctuation [24]. We note that there are some papers reporting ‘weak correlations’ in these compounds [20, 33, 43, 46]. It apparently seems contrary but we have to be careful that some reports support ‘weaker than Fe-based compounds’ [46] while other ‘weaker correlation in XC potentials’. [20, 33] These are therefore not necessarily contrary to the present statement that ‘the correlation gets stronger to overwhelm the conventional electron-phonon mechanism’. The above exotic orbital orderings [24, 43] are reported to be possible even when ‘the correlation is weak’, but again we wonder if this would be such a situation as $E_{corr}^{Fe} > E_{corr}^{Ti} > E_{ph.}$, where $E_{corr.}$ and $E_{ph.}$ correspond to the typical energy scale of electronic correlations and electron-phonon interaction, respectively. Though the superconductivities in $BaTi_2Pn_2O$ ($Pn = Sb, Bi$) have been thought to be conventional BCS type [15–18], the present result implies the possibility of some exotic superconducting mechanism with heavier Pn . We also note that it was pointed out [26] that the superconductivity in $Ba_{1-x}Na_xTi_2Sb_2O$ is at the verge of unconventional superconductivity by the Uemura classification scheme [25].

IV. CONCLUSION

We performed *ab-initio* phonon calculations for $Na_2Ti_2Pn_2O$ ($Pn = As, Sb$) to investigate if the experimentally observed superlattice peaks can be explained by negative frequency modes. For $Pn = As$, we obtained a $C2/m$ (monoclinic No.12) superlattice that is completely consistent with the experimentally observed structure. The consistency indicates that simple electron-phonon interaction can explain the phase transition for $Pn = As$. On the other hand, we obtained a $Cmce$ (orthorhombic No.64) superlattice for $Pn = Sb$ that is inconsistent with the experimentally observed structure $Cmcm$ (orthorhombic No.63). The discrepancy would be intrinsic so that it should be accounted for by those mechanism beyond electron-phonon interaction, such

as strong electronic correlations. Such a discrepancy is also found in superconducting $BaTi_2Pn_2O$ when the pnictogen gets heavier. These facts imply a systematic dependence on pnictogen to tune the mechanism of the phase transition and superconductivity from conventional to exotic.

ACKNOWLEDGMENTS

The computation in this work has been mainly performed using the facilities of the Center for Information Science in JAIST. K.H. is grateful for financial support from a KAKENHI grant (15K21023), a Grant-in-Aid for Scientific Research on Innovative Areas (16H06439), PRESTO and the Materials research by Information Integration Initiative (MI²I) project of the Support Program for Starting Up Innovation Hub from Japan Science and Technology Agency (JST). R.M. is grateful for financial support from MEXT-KAKENHI grants 26287063 and that from the Asahi glass Foundation.

APPENDIX A : ELECTRONIC STRUCTURES

We described electronic structures for undistorted $Na_2Ti_2Pn_2O$ ($Pn = As, Sb$) structure in order to carefully examine the artifacts due to the choice of pseudo potentials (PP). The obtained electronic structures shown in Fig. 6 are consistent with the previous calculations [33, 47].

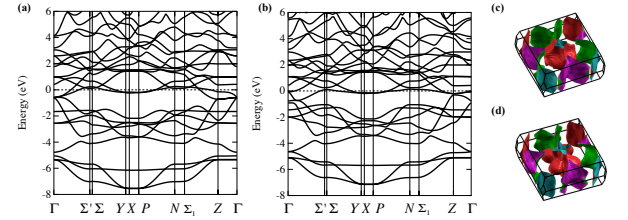


FIG. 6. Band structures and Fermi surfaces for undistorted $Na_2Ti_2Pn_2O$ structure ((a) and (c) $Pn = As$, (b) and (d) $Pn = Sb$)

APPENDIX B : BRILLOUIN ZONES

The primitive Brillouin zone for undistorted $Na_2Ti_2Pn_2O$ ($I4/mmm$) is shown in Fig. 7 (a). The special k and q points are $\Gamma = (2\pi/a) \cdot (0, 0, 0)$, $N = (2\pi/a) \cdot (1/2, 0, a/2c)$, $P = (2\pi/a) \cdot (1/2, 1/2, a/2c)$, $X = (2\pi/a) \cdot (1/2, 1/2, 0)$, $\Sigma' = (2\pi/a) \cdot (1/2, 0, 0)$, $Z = (2\pi/a) \cdot (0, 0, a/c)$ in cartesian axis, where a and c are conventional lattice constants for the undistorted structures. The primitive Brillouin zone for $Na_2Ti_2Sb_2O$ superlattice ($Cmce$) is also shown in Fig. 7 (b). The special k and q points are $\Gamma = (2\pi/a') \cdot (0, 0, 0)$, $X = (2\pi/a') \cdot (1, 0, 0)$, $S = (2\pi/a') \cdot (1/2, a'/2b', 0)$, $Z = (2\pi/a') \cdot (0, 0, a'/2c')$, $A = (2\pi/a') \cdot (1, 0, a'/2c')$, $R = (2\pi/a') \cdot (1/2, a'/2b', a'/2c')$ in cartesian axis, where a' , b' and c' are conventional lattice constants for the superlattice structure.

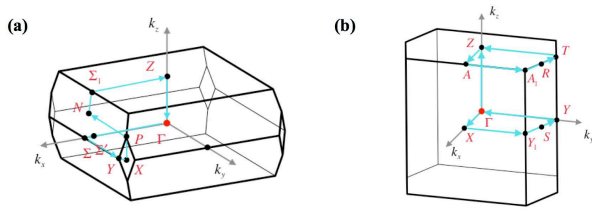


FIG. 7. Primitive Brillouin zones (a) for undistorted $\text{Na}_2\text{Ti}_2\text{Pn}_2\text{O}$ structure ($I4/mmm$) and (b) for $\text{Na}_2\text{Ti}_2\text{Sb}_2\text{O}$ superlattice ($Cmce$).

APPENDIX C : GEOMETRY OPTIMIZATIONS

The results of geometry optimizations are shown in Table I-III. The conventional lattice vectors of the superlattice structure for $Pn = \text{As}$ ($C2/m$) are redefined as $\vec{d}' = 2(\vec{a} - \vec{b})$, $\vec{b}' = 2(\vec{a} + \vec{b})$ and $\vec{c}' = 1/2(-\vec{a} + \vec{b} + \vec{c})$, those for $Pn = \text{Sb}$ ($Cmce$) are redefined as $\vec{d}' = \vec{c}$, $\vec{b}' = (\vec{a} - \vec{b})$ and $\vec{c}' = (\vec{a} + \vec{b})$, and those for $Pn = \text{Sb}$ ($Cmcm$) are redefined as $\vec{d}' = 2(\vec{a} + \vec{b})$, $\vec{b}' = 2(\vec{b} - \vec{a})$ and $\vec{c}' = \vec{c}$, where \vec{a} , \vec{b} and \vec{c} are conventional lattice vectors of the undistorted structures.

TABLE I. The results of geometry optimization for undistorted $\text{Na}_2\text{Ti}_2\text{Pn}_2\text{O}$ structure ($Pn = \text{As, Sb}$). The relaxed conventional lattice parameters are $a = 4.071128 \text{ \AA}$, $c = 15.440517 \text{ \AA}$, ($a = 4.13957 \text{ \AA}$, $c = 16.97766 \text{ \AA}$) for $Pn = \text{As}$ (Sb). The final enthalpy is -980.0514 Ry (-1323.3103 Ry) for $Pn = \text{As}$ (Sb) per formula unit [$\text{Na}_2\text{Ti}_2\text{Pn}_2\text{O}$].

$Pn = \text{As} (I4/mmm)$				
label	x	y	z	wyckoff
Na	0.50000	0.50000	0.18146	4e
Ti	0.50000	0.00000	0.00000	4c
As	0.00000	0.00000	0.11752	4e
O	0.50000	0.50000	0.00000	2b

$Pn = \text{Sb} (I4/mmm)$				
label	x	y	z	wyckoff
Na	0.50000	0.50000	0.18369	4e
Ti	0.50000	0.00000	0.00000	4c
Sb	0.00000	0.00000	0.12015	4e
O	0.50000	0.50000	0.00000	2b

For $Pn = \text{As}$ ($C2/m$), we need to take special care when comparing our calculated geometry with an experimental one due to Davis et al.[28] We found that the atomic positions listed in their Table I are incompatible with their superlattice vectors, $\vec{d}' = 2(\vec{a} + \vec{b})$, $\vec{b}' = 2(\vec{b} - \vec{a})$, and $\vec{c}' = 1/2(\vec{a} + \vec{b} + \vec{c})$, described in their main text [28]: (1) If the description in the main text is assumed to be correct, Na and Sb positions in the superlattice are respectively located unlikely far from their undistorted positions. (2) O is not located at (0,0,0) in their Fig. 6 (a), being inconsistent with their Table I. Accordingly, we speculate that they again define the superlattice vectors compatible with the atomic positions in their Table I, which differs from that in their main text. We

also found $y = 0.0$ for As3 in their Table I must be a typo and correctly $y = 0.25$ because As3 should occupy 8j Wyckoff site and its undistorted position is $y = 0.5$. Assuming our speculation is correct, our optimized geometry parameters agree well with their experimental values.

TABLE II. The results of geometry optimization for $\text{Na}_2\text{Ti}_2\text{Pn}_2\text{O}$ superlattice ($Pn = \text{As, Sb}$) obtained by phonon calculations. The conventional lattice parameters after relaxation are $a' = 11.51310 \text{ \AA}$, $b' = 11.51244 \text{ \AA}$, $c' = 8.23431 \text{ \AA}$, $\beta = 110.45774^\circ$ ($a' = 17.04343 \text{ \AA}$, $b' = 5.83920 \text{ \AA}$, $c' = 5.83039 \text{ \AA}$) for $Pn = \text{As}$ (Sb). The final enthalpy is -980.0517 Ry (-1323.3120 Ry) for $Pn = \text{As}$ (Sb) per formula unit [$\text{Na}_2\text{Ti}_2\text{Pn}_2\text{O}$].

$Pn = \text{As} (C2/m)$				
label	x	y	z	wyckoff
Na	0.90907	0.00000	0.63699	4i
Na	0.40943	0.00000	0.63694	4i
Na	0.15932	0.24981	0.63725	8j
Ti	0.13031	0.11979	0.00000	8j
Ti	0.88019	0.36969	0.00000	8j
As	0.80877	0.00000	0.23625	4i
As	0.30933	0.00000	0.23625	4i
As	0.05905	0.24969	0.23623	8j
O	0.00000	0.00000	0.00000	2a
O	0.25000	0.25000	0.00000	4e
O	0.00000	0.50000	0.00000	2b

$Pn = \text{Sb} (Cmce)$				
label	x	y	z	wyckoff
Na	0.18411	0.00000	0.00000	8d
Ti	0.00000	0.23266	0.26812	8f
Sb	0.37883	0.00000	0.00000	8d
O	0.00000	0.00000	0.00000	4a

TABLE III. The results of geometry optimization for experimentally observed $\text{Na}_2\text{Ti}_2\text{Sb}_2\text{O}$ superlattice. The conventional lattice parameters after relaxation are $a' = 11.73782 \text{ \AA}$, $b' = 11.73541 \text{ \AA}$, and $c' = 16.82525 \text{ \AA}$. The final enthalpy is -1323.3109 Ry per formula unit [$\text{Na}_2\text{Ti}_2\text{Sb}_2\text{O}$].

$Pn = \text{Sb} (Cmcm)$				
label	x	y	z	wyckoff
Na	0.00000	0.37498	0.93293	8f
Na	0.00000	0.12503	0.43294	8f
Na	0.74999	0.12500	0.93275	16h
Ti	0.37417	0.00083	0.25000	8g
Ti	0.62584	0.24918	0.25000	8g
Ti	0.87581	-0.00085	0.25000	8g
Ti	0.12418	0.25082	0.25000	8g
Sb	0.00000	0.37533	0.12909	8f
Sb	0.00000	0.12532	0.62908	8f
Sb	0.75033	0.12499	0.12907	16h
O	0.00000	0.62500	0.25000	4c
O	0.00000	0.12500	0.25000	4c
O	0.75000	0.37500	0.25000	8g

-
- [1] E. A. III, T. Ozawa, S. M. Kauzlarich, and R. R. Singh, *Journal of Solid State Chemistry* **134**, 423 (1997).
- [2] T. C. Ozawa, S. M. Kauzlarich, M. Bieringer, , and J. E. Greedan, *Chemistry of Materials* **13**, 1804 (2001).
- [3] R. H. Liu, D. Tan, Y. A. Song, Q. J. Li, Y. J. Yan, J. J. Ying, Y. L. Xie, X. F. Wang, and X. H. Chen, *Phys. Rev. B* **80**, 144516 (2009).
- [4] X. F. Wang, Y. J. Yan, J. J. Ying, Q. J. Li, M. Zhang, N. Xu, and X. H. Chen, *Journal of Physics: Condensed Matter* **22**, 075702 (2010).
- [5] P. Doan, M. Gooch, Z. Tang, B. Lorenz, A. Moller, J. Tapp, P. C. W. Chu, and A. M. Guloy, *Journal of the American Chemical Society* **134**, 16520 (2012).
- [6] T. Yajima, K. Nakano, F. Takeiri, T. Ono, Y. Hosokoshi, Y. Matsushita, J. Hester, Y. Kobayashi, and H. Kageyama, *Journal of the Physical Society of Japan* **81**, 103706 (2012).
- [7] T. Yajima, K. Nakano, F. Takeiri, J. Hester, T. Yamamoto, Y. Kobayashi, N. Tsuji, J. Kim, A. Fujiwara, and H. Kageyama, *Journal of the Physical Society of Japan* **82**, 013703 (2013).
- [8] T. Yajima, K. Nakano, F. Takeiri, Y. Nozaki, Y. Kobayashi, and H. Kageyama, *Journal of the Physical Society of Japan* **82**, 033705 (2013).
- [9] H.-F. Zhai, W.-H. Jiao, Y.-L. Sun, J.-K. Bao, H. Jiang, X.-J. Yang, Z.-T. Tang, Q. Tao, X.-F. Xu, Y.-K. Li, C. Cao, J.-H. Dai, Z.-A. Xu, and G.-H. Cao, *Phys. Rev. B* **87**, 100502 (2013).
- [10] K. Nakano, T. Yajima, F. Takeiri, M. A. Green, J. Hester, Y. Kobayashi, and H. Kageyama, *Journal of the Physical Society of Japan* **82**, 074707 (2013).
- [11] U. Pachmayr and D. Johrendt, *Solid State Sciences* **28**, 31 (2014).
- [12] F. von Rohr, R. Nesper, and A. Schilling, *Phys. Rev. B* **89**, 094505 (2014).
- [13] J. Bednorz and K. Müller, *Zeitschrift für Physik B Condensed Matter* **64**, 189 (1986).
- [14] Y. Kamihara, T. Watanabe, M. Hirano, , and H. Hosono, *Journal of the American Chemical Society* **130**, 3296 (2008).
- [15] A. Subedi, *Phys. Rev. B* **87**, 054506 (2013).
- [16] F. von Rohr, A. Schilling, R. Nesper, C. Baines, and M. Bendele, *Phys. Rev. B* **88**, 140501 (2013).
- [17] S. Kitagawa, K. Ishida, K. Nakano, T. Yajima, and H. Kageyama, *Phys. Rev. B* **87**, 060510 (2013).
- [18] Y. Nozaki, K. Nakano, T. Yajima, H. Kageyama, B. Frandsen, L. Liu, S. Cheung, T. Goko, Y. J. Uemura, T. S. J. Munsie, T. Medina, G. M. Luke, J. Munevar, D. Nishio-Hamane, and C. M. Brown, *Phys. Rev. B* **88**, 214506 (2013).
- [19] M. Gooch, P. Doan, Z. Tang, B. Lorenz, A. M. Guloy, and P. C. W. Chu, *Phys. Rev. B* **88**, 064510 (2013).
- [20] S. Tan, J. Jiang, Z. Ye, X. Niu, Y. Song, C. Zhang, P. Dai, B. Xie, X. Lai, and D. Feng, *arXiv preprint arXiv:1505.01915* (2015).
- [21] B. A. Frandsen, E. S. Bozin, H. Hu, Y. Zhu, Y. Nozaki, H. Kageyama, Y. J. Uemura, W.-G. Yin, and S. J. L. Billinge, *Nat Commun* **5**, 5761 (2014).
- [22] M. J. Lawler, K. Fujita, J. Lee, A. R. Schmidt, Y. Kohsaka, C. K. Kim, H. Eisaki, S. Uchida, J. C. Davis, J. P. Sethna, and E.-A. Kim, *Nature* **466**, 347 (2010).
- [23] K. Fujita, M. H. Hamidian, S. D. Edkins, C. K. Kim, Y. Kohsaka, M. Azuma, M. Takano, H. Takagi, H. Eisaki, S.-i. Uchida, A. Allais, M. J. Lawler, E.-A. Kim, S. Sachdev, and J. C. S. Davis, *Proceedings of the National Academy of Sciences* **111**, E3026 (2014).
- [24] H. Nakaoka, Y. Yamakawa, and H. Kontani, *Phys. Rev. B* **93**, 245122 (2016).
- [25] Y. J. Uemura, L. P. Le, G. M. Luke, B. J. Sternlieb, W. D. Wu, J. H. Brewer, T. M. Riseman, C. L. Seaman, M. B. Maple, M. Ishikawa, D. G. Hinks, J. D. Jorgensen, G. Saito, and H. Yamochi, *Phys. Rev. Lett.* **66**, 2665 (1991).
- [26] S. Kamusella, P. Doan, T. Goltz, H. Luetkens, R. Sarkar, A. Guloy, and H.-H. Klauss, in *Journal of Physics: Conference Series*, Vol. 551 (IOP Publishing, 2014) p. 012026.
- [27] K. Nakano, K. Hongo, and R. Maezono, *Scientific Reports* **6** (2016).
- [28] N. R. Davies, R. D. Johnson, A. J. Princep, L. A. Gannon, J.-Z. Ma, T. Qian, P. Richard, H. Li, M. Shi, H. Nowell, P. J. Baker, Y. G. Shi, H. Ding, J. Luo, Y. F. Guo, and A. T. Boothroyd, *Phys. Rev. B* **94**, 104515 (2016).
- [29] D. Chen, T.-T. Zhang, Z.-D. Song, H. Li, W.-L. Zhang, T. Qian, J.-L. Luo, Y.-G. Shi, Z. Fang, P. Richard, *et al.*, *Physical Review B* **93**, 140501 (2016).
- [30] K. Kuroki, H. Usui, S. Onari, R. Arita, and H. Aoki, *Phys. Rev. B* **79**, 224511 (2009).
- [31] T. Miyake, K. Nakamura, R. Arita, and M. Imada, *Journal of the Physical Society of Japan* **79**, 044705 (2010).
- [32] D. J. Singh, *New Journal of Physics* **14**, 123003 (2012).
- [33] X.-W. Yan and Z.-Y. Lu, *Journal of Physics: Condensed Matter* **25**, 365501 (2013).
- [34] J. P. Perdew, K. Burke, and M. Ernzerhof, *Phys. Rev. Lett.* **77**, 3865 (1996).
- [35] P. Giannozzi, S. Baroni, N. Bonini, M. Calandra, R. Car, C. Cavazzoni, D. Ceresoli, G. L. Chiarotti, M. Cococcioni, I. Dabo, A. D. Corso, S. de Gironcoli, S. Fabris, G. Fratesi, R. Gebauer, U. Gerstmann, C. Gougoussis, A. Kokalj, M. Lazzeri, L. Martin-Samos, N. Marzari, F. Mauri, R. Mazzarello, S. Paolini, A. Pasquarello, L. Paulatto, C. Sbraccia, S. Scandolo, G. Sclauzero, A. P. Seitsonen, A. Smogunov, P. Umari, and R. M. Wentzcovitch, *Journal of Physics: Condensed Matter* **21**, 395502 (2009).
- [36] P. E. Blöchl, *Phys. Rev. B* **50**, 17953 (1994).
- [37] F. Jollet, M. Torrent, and N. Holzwarth, *Computer Physics Communications* **185**, 1246 (2014).
- [38] E. Kucukbenli, M. Monni, B. Adetunji, X. Ge, G. Adebayo, N. Marzari, S. de Gironcoli, and A. D. Corso, *arXiv* **1404**, 3015 (2014).
- [39] S. Baroni, S. de Gironcoli, A. Dal Corso, and P. Giannozzi, *Rev. Mod. Phys.* **73**, 515 (2001).
- [40] K. Momma and F. Izumi, *Journal of Applied Crystallography* **44**, 1272 (2011).
- [41] A. Kokalj, *Journal of Molecular Graphics and Modelling* **17**, 176 (1999).
- [42] N. Marzari, D. Vanderbilt, A. De Vita, and M. C. Payne, *Phys. Rev. Lett.* **82**, 3296 (1999).
- [43] H.-S. Kim and H.-Y. Kee, *Physical Review B* **92**, 235121 (2015).
- [44] T. C. Ozawa, R. Pantoja, E. A. Axtell, S. M. Kauzlarich, J. E. Greedan, M. Bieringer, and J. W. Richardson, *Journal of Solid State Chemistry* **153**, 275 (2000).
- [45] R. Liu, Y. Song, Q. Li, J. Ying, Y. Yan, Y. He, and X. Chen, *Chemistry of Materials* **22**, 1503 (2010).
- [46] Y. Huang, H. Wang, W. Wang, Y. Shi, and N. Wang, *Physical Review B* **87**, 100507 (2013).
- [47] D. Suetin and A. Ivanovskii, *Journal of Alloys and Compounds* **564**, 117 (2013).